Simultaneous Simulation of Gas Diffusion Layer and Air Channel in a Polymer Electrolyte Membrane Fuel Cell: Pore-Scale Modeling of Water Flooding

E. Shakerinejad, M. Nazari, M. H. Kayhani

Department of Mechanical Engineering, Shahrood University of Technology, Shahrood, Iran

ABSTRACT: In this study, Lattice Boltzmann method is used to investigate liquid water transport in a carbon paper gas diffusion layer and gas channel of polymer electrolyte membrane fuel cells. The effects of gas diffusion layer wettability on the removal process and liquid water distribution are investigated. In addition, liquid water dynamic behaviors and liquid water saturation within the gas diffusion layer in two case of steady and transient are explored. This study focuses on the effects of surface wettability on the number of effective clusters, merging of clusters, and the required time for reaching the steady-state water distribution. The results show that the wettability of surface affects on the saturation of liquid water in the gas diffusion layer and in 100lu<Y<160lu, this effect is noticeable. The steady-state water distribution is observed at time step of 1590000 and 1500000 (lattice unit) for the contact angles of 115° and 145°, respectively. Thus the simulation results show that by increasing the contact angle of fibers in gas diffusion layer, the required time to obtain a steady state water distribution is reduced. Therefore, if the solid surface becomes more hydrophobic, water management will be improved in the gas diffusion layer.

1- Introduction

Fuel cells are efficient energy conversion devices which directly convert the chemical energy stored in a fuel into electrical energy through electrochemical reactions [1]; thus, fuel cells are clean and more efficient than the conventional heat engines. Among the many fuel cell technologies, Polymer Electrolyte Membrane Fuel Cells (PEMFCs) have higher efficiencies and energy densities and are capable of rapidly adjusting to power demands [2, 3].

Poor water management in a PEMFC results in either flooding phenomenon or membrane hydrations [4]. If excessive liquid water accumulates in the components of a PEMFC including Gas Channel (GC), Gas Diffusion Layer (GDL), and Catalyst Layer (CL), flooding problems occur [5]. Flooding is a result of continuous generation of water in the cathode side [6]. Thus when flooding phenomenon occurs, liquid water fills pores of cathode gas diffusion layer and catalyst layer and hinders the effective transport of oxygen to the CL, leading to reactant starvation and performance loss [4]. On the other hand, membrane dehydration increases the proton conductive resistance and thus reduces the cell performance owing to great ohmic loss across the membrane [5]. The transport of liquid water within the GDL is one of the most important water management issues in PEMFC [5]. The GDL plays a critical role in the water management

*Corresponding author;s email: mnazari@shahroodut.ac.ir

which maintains the delicate balance between water removal and membrane hydration [7]. Carbon-fiber based porous structure, such as carbon paper and carbon cloth are the most commonly used materials for the GDL. The GDL is naturally hydrophilic. In order to facilitate the removal of liquid water, GDL is usually treated with a non-wetting polymer such as PolyTetraFluoroEthylene (PTFE) to make them hydrophobic [5]. The transport of liquid water through a GDL is a drainage process in which the non-wetting liquid water displaces the wetting air. The displacement is dominated by capillary forces due to the low water flow rate and narrow void space within the GDL [5]. In the cathode of a PEMFC, liquid water generated in the CL penetrates through the GDL and finally enters the GC [5]. In this study, effects of GDL contact angle on the dynamic transport of liquid water are investigated.

2- Numerical Method

The contact angles for the solid particles in the GDL are set to 115°, or 145° [8, 9]. A cross-section of the 3D reconstructed GDL is selected and serves as the 2D porous GDL in the computational domain to simulate liquid water transport in PEMFCs, as shown in Fig. 1. The thickness of the GDL is 400 μm and a 300 μm high gas channel is added at the top of it. The calculation domain is rectangular with dimensions of $2000\Delta x \times 700\Delta x$. Here, the length of physical unit, Δx, is set to 1μm. In Fig. 1, a GDL layer is generated by randomly
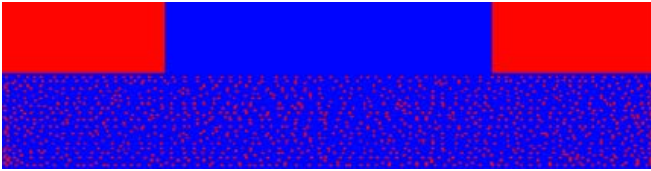
Fig. 1. Schematic diagram of the computational domain. The calculation domain is rectangular with dimensions of 2000Δx × 700Δx. The thickness of the GDL is 400 μm and a 300 μm high gas channel is added at the top of it.

placing circular solid particles in a layer with a thickness of $400\Delta x$. A porosity of 0.88 and particle diameter of 10 *lu* are used for the simulation of the GDL. The contact angle for the GDL particles is set to 115°, or 145° and slightly hydrophobic rib with a contact angle of 110° is considered in the present study. At the bottom boundary, liquid water is injected into the GDL with an inflowing velocity of 7.877×10^{-5} in lattice unit and the resulting Reynolds number is 0.004725. The capillary number of the present simulations is 6×10^{-5}, which is small enough to ensure capillary-dominant liquid water transport. The boundary conditions proposed by Zou and He, who implemented them on the inlet boundary, are applied.

We implement the Shan-Chen (S–C) model for a multicomponent multiphase system. The so-called D_2Q_9 model is used in this work, in which D_2 indicates two dimensions, and Q_9 means the nine corresponding velocity directions.

3- Results and Discussion

The water liquid saturation (*S*) versus time (*t*) in the GDL is shown in Fig. 2. Water liquid saturation is defined as the ratio of water liquid volume to void volume.

According to Fig.2, this graph shows two different parts: 1) the linear increment of *S* versus time and 2) the flat section. The first section is related to the penetration of water inside the GDL before formation of droplets in the area of GC. In this case, the flow rate from the outlet surface (to GC) is zero and the time variation of mass inside the GDL is equal to the inlet mas flow rate. So, this part of the graph is linear with a positive and constant slope. In the second part of the graph, the droplets are formed in the GC and the liquid clustered are reached to the GC. In this condition, the variations of mass inside the GDL become zero and therefore; a relatively flat
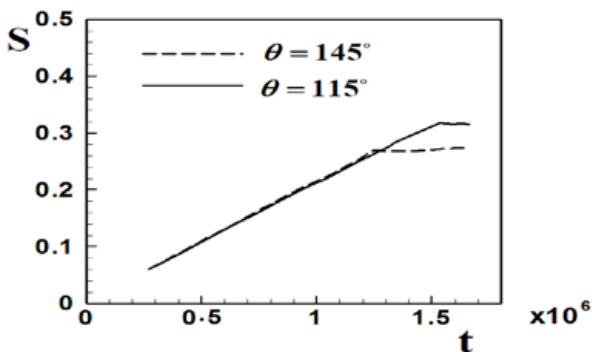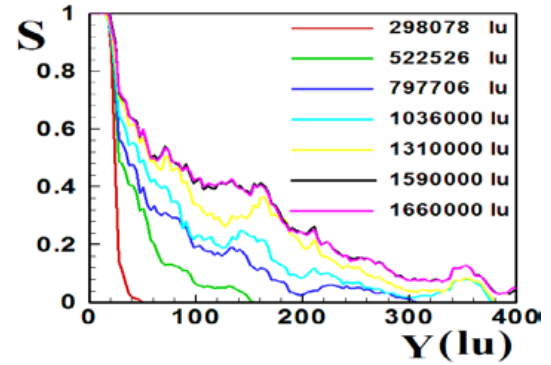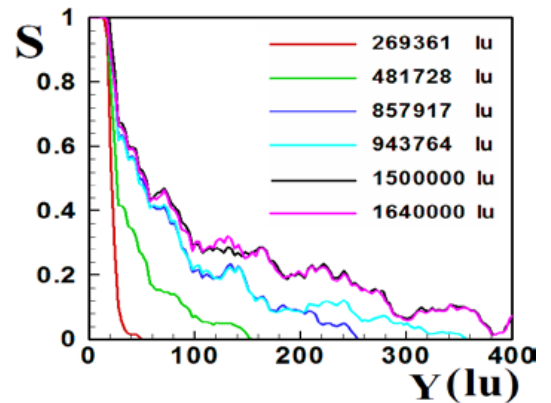

(a)

(b)

Fig. 3. Evolution of liquid water clusters in a GDL with different contact angles: (a) contact angle of 115°, and (b) contact angle of 145°.

curve is appeared in this saturation level inside the GDL. In the steady-state, the mass flow rates are the same in outlet and inlet boundaries. In *S-t* graph, the global measurement of water inside the GDL is measured versus time. In other word, the total volume of water inside the GDL is calculated.

The evolution of the liquid water distribution in the GDL is investigated with the water saturation profile at several simulation times, as shown in Fig. 3.

This figure indicates evolution of the cross sectional liquid water saturation along the Y direction of the GDL. The cross sectional water liquid saturation is defined as the ratio of the area occupied by water to the total pore area in each cross-section. Different colored curves indicate different simulation times of dynamic liquid water. As shown, the saturation distribution inside the GDL becomes fully developed at 1590000 and 1500000 *lu* time for the contact angle of 115° and 145°, respectively. Fig. 3 shows that the saturation distribution inside the GDL is continuously increased until the breakthrough droplets are formed in the GC and reaches to the steady-state saturation level.

4. Conclusion

As shown in Fig. 2 by employing more hydrophobic PTLs, the steady-state saturation level in the GDL is decreased. As the solid surface becomes more hydrophobic, the time required to arrive at a steady-state water distribution is reduced, indicating faster removal of liquid water from the GDL to the GC and improved water management.

Fig. 2. The water liquid saturation (S) versus time (t) in the GDL for the contact angle of 115° and145°.

References

[1] Molaeimanesh, G., and Akbari, M.H., 2014. "Water droplet dynamic behavior during removal from a proton exchange membrane fuel cell gas diffusion layer by Lattice-Boltzmann method". *Korean J. Chem. Eng*, 31(4), PP. 598-610.

[2] O'Hayre, R., Cha, S.W., Colella, W., and Prinz, F.B., 2009. *"Fuel Cell Fundamentals"*. Second ed., John Wiley & Sons.

[3] Wang, C.Y., 2004. "Fundamental models for fuel cell engineering". *Chem. Rev*, 104, PP. 4727-4766.

[4] Chen, L., Luan, H.B., and Tao, W.Q., 2010. "Liquid water dynamic behaviors in the GDL and GC of PEMFCS using lattice Boltzmann method". *Frontiers in Heat and Mass Transfer* (FHMT), 1, 023002.

[5] Chen, L., Luan, H.B., He, Y.L., and Tao, W.Q., 2012. "Numerical Investigation of Liquid Water Transport and Distribution in Porous Gas Diffusion Layer of a Proton Exchange Membrane Fuel Cell Using Lattice Boltzmann Method". *Published in Russian in Elektrokhimiya*, Vol. 48, No. 7, pp. 786–800.

[6] Tamayol, A., and Bahrami, M., 2011 "Water permeation through gas diffusion layers of proton exchange membrane fuel cells". *Journal of Power Sources,* 196, pp. 6356–6361.

[7] Li, H., Tang, Y., Wang, Z., Shi, Z., Wu, S., Song, D., Zhang, J., Fatih, K., Zhang, J., Wang, H., Liu, Z., Abouatallah, R. and Mazza, A., 2008, "A review of water flooding issues in the proton exchange membrane fuel cell". *Journal of Power Sources*, 178(1), PP. 103-117.

[8] Hao, L., and Cheng, P., 2010. "Lattice Boltzmann simulations of water transport in gas diffusion layer of a polymer electrolyte membrane fuel cell". *Journal of Power Sources*, 195, pp. 3870–3881.

[9] Hao, L., and Cheng, P., 2010, "Pore-scale simulations on relative permeabilities of porous media by lattice Boltzmann method". *International Journal of Heat and Mass Transfer*, 53, pp. 1908–1913.